Evaluation of an Olefin Metathesis Pre-catalyst with a Bulky and Electron-Rich N-Heterocyclic Carbene

Simone Manzini,[a] César A. Urbina Blanco,[a†] David J. Nelson,[a‡] Albert Poater,[b] Tomas Lebl,[a] Sébastien Meiries,[a] Alexandra M. Z. Slawin,[a] Laura Falivene,[c] Luigi Cavallo[c,d] and Steven P. Nolan[a]*

[a] EaStCHEM School of Chemistry, University of St Andrews, North Haugh, St Andrews, Fife, KY16 9ST, UK. [b] Institut de Química Computacional i Catàlisi and Departament de Química, Universitat de Girona, Campus Montilivi, 17071 Girona, Catalonia, Spain. [c] KAUST Catalyst Center, Physical Sciences and Engineering Division, King Abdullah University of Science and Technology, Thuwal 23955-6900, Saudi Arabia. [d] Department of Chemistry and Biology, University of Salerno, Via Ponte don Melillo, Fisciano I-84084, Italy. * Steven P. Nolan: snolan@st-andrews.ac.uk. [†] Current address for SM: Catalysis Research Laboratory (CaRLa), Im Neuenheimer Feld 584, 69120 Heidelberg, Germany. [‡] Current address for CAUB: Lehrstuhl für Technische Chemie und Petrolchemie, Institut für Technische und Makromolekulare Chemie (ITMC), RWTH Aachen University, Worringerweg 1, 52074 Aachen, Germany. ^ Current address for DJN: WestCHEM Department of Pure and Applied Chemistry, University of Strathclyde, 295 Cathedral Street, Glasgow, G1 1XL, UK.

Abstract

The commercially-available metathesis pre-catalyst $\mathbf{M_{23}}$ has been evaluated alongside new complex [$RuCl_2$((3-phenyl)indenylidene)(PPh_3)($SIPr^{OMe}$)] (**1**), which bears a *para*-methoxy-substituted *N*-heterocyclic carbene ligand. Several model metathesis reactions could be conducted using only parts-per-million levels of ruthenium catalyst. The effects of the different NHC ligands on reactivity have been explored.

Introduction

N-heterocyclic carbenes (NHCs) are one of the most important types of ligand in modern organometallic chemistry.[1, 2] To allow the fine-tuning of the electronic[3] and steric[4] properties affecting the catalytic properties of the metal centres to which they are co-ordinated, numerous NHC ligands have been reported in the literature.[5] In particular, NHCs have played key roles in gold[6] and palladium[7] catalysis, and have proved to be a breakthrough in ruthenium-catalysed olefin metathesis.[8-

[10] Indeed, since the introduction of heteroleptic NHC-phosphine ruthenium olefin metathesis catalysts[11, 12] (e.g. **Figure 1**), they have surpassed the activity of the previous generations of bis(phosphine) complexes.[13, 14] This improvement is due to factors such as the increased affinity of the 14e$^-$ species for alkene over phosphine,[15] the lower energy differences between active and inactive η^2-complexes,[16] and the increased stability of the alkylidenes.[17]

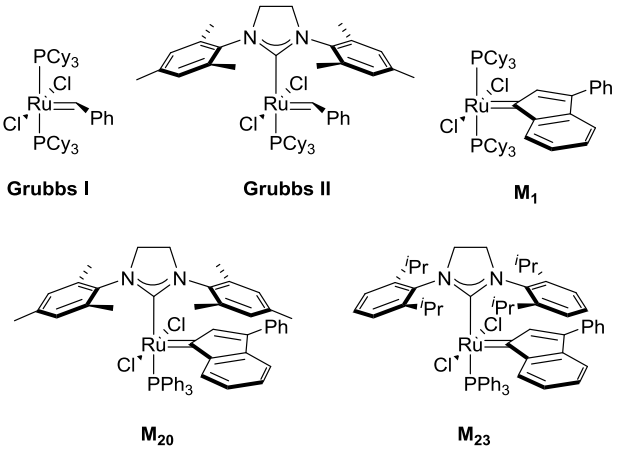

Figure 1. Common commercially-available pre-catalysts.

The required ligand sphere for a given olefin metathesis reaction can vary considerably, depending on the needs of the reaction to be catalysed.[14] In particular, by tuning the electronic and steric properties of the NHC ligand, it is possible to modulate the reactivity of the catalyst, taking into account the structure of the substrates. However, it is not always easy to predict how a structural change at the NHC can affect olefin metathesis activity. For example, when IMes is compared to its bulkier analogue IPr (which bears two *iso*propyl substituents on the *N*-aryl moiety), the latter shows higher catalytic activity. If IPr and the saturated analogue SIPr are compared, there is a considerable difference in reactivity, with the latter affording metathesis at very low catalyst loadings.[18, 19] A similar trend is apparent between IMes and SIMes, but there is not yet a simple explanation for why saturated NHCs are better ligands for olefin metathesis catalysts. Further investigation of the effect of ligand properties on metathesis catalyst activity are therefore required, which can often be explored by systematic changes to the ligand sphere. The use of established metrics such as TEP[20] and percent buried volume ($\%V_{bur}$)[4, 21] can allow ligand properties to be quantified, while the measurement of the rates of key processes[22] such as initiation allows some insight into which aspects of the reaction mechanism are affected by these changes. Methoxy-functionalised NHCs[23] have been shown to be excellent ligands for palladium catalysts, compared to the corresponding parent NHCs.[24, 25] Plenio has synthesised a range of *para*-substituted (S)IMes derivatives and explored their properties by various spectroscopic and electrochemical means, and established that *para*-substitution of the NHC ligand does indeed affect the properties of the transition metal centre.[26] We therefore wished to explore their

use as ligands for metathesis pre-catalysts, comparing **1** with the recently discovered and already commercially available **M$_{23}$**; while only a preliminary evaluation of the catalytic activity of the latter has been disclosed, it has shown very high activity in olefin metathesis, and a full evaluation of its properties is warranted.

Results and Discussion

Synthesis and Characterisation of [RuCl$_2$((3-phenyl)indenylidene)(PPh$_3$)(SIPrOMe)] (1)

We have previously reported the synthesis, characterisation, and catalytic testing of [RuCl$_2$((3-phenyl)indenylidene)(PPh$_3$) (SIPr)] (**M$_{23}$**).[18, 27] This complex shows promising activity in RCM and CM with less hindered substrates, reaching full conversion at 1 mol% of catalyst loading in only 0.5 h. However, the complex is not capable of promoting metathesis transformations with more hindered substrates.

New complex **1** was prepared in order to investigate how modulating the electronic nature of the aryl ring, with minimal steric changes, might affect the catalytic activity of the resulting complex. The synthesis and characterisation of SIPr^{OMe} have been previously reported by us;[23, 28] it was found that it typically has a similar steric impact to SIPr, but is slightly more σ-donating and less π-accepting. Using a method analogous to the reported procedure for the synthesis of **M$_{23}$**,[27] complex **1** was obtained in 82% yield as an analytically-pure red solid (**Scheme 1**). This new complex was characterised by ^{1}H, ^{13}C{^{1}H}, and ^{31}P{^{1}H} NMR spectroscopy (see the Supporting Information).

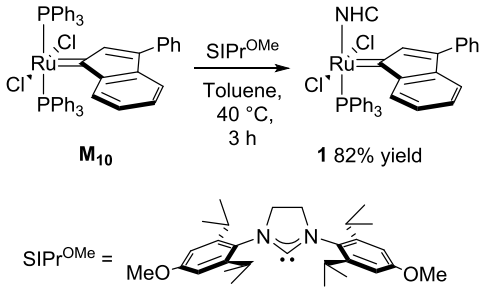

Scheme 1. Synthesis of complex 1.

In order to evaluate the steric impact of the NHC in each complex, crystals suitable for X-ray diffraction analysis were obtained by slow diffusion of pentane into a concentrated dichloromethane solution. Representations of these crystal structures can be found in **Figure 2**, while key structural properties of each complex, plus those of [RuCl$_2$((3-phenyl)indenylidene)(PPh$_3$)(IPr)] (**2**),[19] are recorded in **Table 1**. Percent buried volumes (%V_{bur})[4] were calculated using the Samb*V*ca web application.[21] The structural features of the three complexes are very similar, with only small differences in Ru-Cl, Ru-C and Ru=C bond lengths. All three complexes exhibit the same distorted

square-based pyramidal geometry. The Ru-P distance in **1** is slightly shorter than in **M$_{23}$**, which may be indicative of increased *d* to π* backbonding in the former complex. The Ru-P distance in **2** is shorter still, which might be attributed to the same effect, as unsaturated NHCs are known to be poorer π-acceptors than the corresponding saturated ligands.[29-32] In complex **1**, the torsion angle in the backbone of the NHC is larger than in **M$_{23}$** by 10°. This difference might be due to the reduced mobility of the aryl ring due to the mesomeric effect of the *para*-methoxy substituent which might force the imidazolium ring into a more distorted conformation. Notably, this is the only structural difference that does not concern the throw-away ligand.

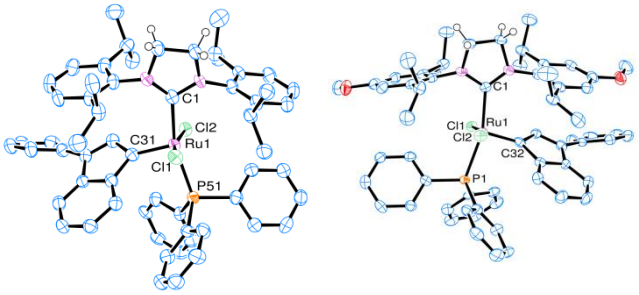

Figure 2. Molecular structures of complexes M$_{23}$ (left) and 1 (right), determined by X-ray crystallographic analysis; thermal ellipsoids are drawn at 50% probability, and H atoms are excluded for clarity.

Table 1. Selected bond lengths (Å) and angles (°) in complexes M$_{23}$, 1 and 2.

Complex		**M$_{23}$**	**1**	**2**
Ru(1)-Cl(1)	(Å)	2.3690(13)	2.3660(11)	2.373(3)
Ru(1)-Cl(2)	(Å)	2.3812(14)	2.3795(11)	2.387(2)
Ru(1)-P(1)	(Å)	2.4204(17)	2.4017(11)	2.368(2)
Ru(1)-C(1)	(Å)	2.092(6)	2.101(4)	2.129(8)
Ru(1)-C(31)	(Å)	1.850(5)	1.850(4)	1.822(7)
Cl(1)-Ru(1)-Cl(2)	(°)	166.38(5)	164.85(4)	166.58(8)
C(1)-Ru(1)-P(1)	(°)	162.30(14)	162.72(11)	164.7(2)
C(1)-Ru(1)-C(31)	(°)	103.1(3)	103.14(15)	102.1(3)
N(2)-C(3)-C(4)-N(5)	(°)	9.8(5)	22.1(4)	1.8(11)
%V$_{bur}$		31.8%	32.0%	31.1%

Pre-catalyst initiation

The pre-catalyst initiation event determines the rate at which the active catalyst is formed during the reaction, and is therefore an important parameter. Recently, we have determined the activation parameters of **M$_{23}$** and other ruthenium indenylidene complexes using [^{31}P, ^{31}P] EXSY experiments,

and kinetic studies of their reactions with butyl vinyl ether.[33] While most complexes initiated *via* a dissociative mechanism (phosphine dissociation to yield a $14e^-$ species, followed by alkene co-ordination), it was found that $\mathbf{M_{20}}$ actually initiates *via* an interchange mechanism (concurrent phosphine dissociation and alkene co-ordination *via* a single transition state). We therefore wished to elucidate whether **1** and **2** initiated *via* the dissociative or interchange mechanism, and how the NHC ligand affects this initiation rate. Notably, interactions between the NHC *N*-aryl substituents and the ruthenium carbene fragment have been postulated to be important to the electronic structure and initiation behaviour of metathesis pre-catalysts.[34-36]

Initiation rates for **1** and **2** were measured using two methods: [^{31}P, ^{31}P] EXSY experiments in the presence of added PPh_3, where the exchange rate of the signals for free and bound phosphine were measured (**Table 2**); and reaction with butyl vinyl ether which irreversibly forms a metathesis-inactive Fischer carbene species[37] under conditions where phosphine dissociation is rate-determining (**Table 3**).[15] Unfortunately, the initiation parameters of **2** could not be measured using the former method due to competing decomposition at the temperatures necessary to effect measurable rates of phosphine exchange. These data reveal that there is very little difference in the activation parameters for the initiation of these complexes. Errors in the entropy measurements are quite large, due to the need to extrapolate to infinite temperature, but enthalpy measurements are slightly more reliable. Complex **2** initiates slightly faster than $\mathbf{M_{23}}$ or **1**, perhaps due to the reduced π-accepting ability of IPr *versus* SIPr or $SIPr^{OMe}$. **1** initiates only very slightly faster than $\mathbf{M_{23}}$, which is consistent with the relatively small difference in TEP between the NHCs on each complex.[23]

Table 2. Activation parameters for $\mathbf{M_{23}}$ and **1** determined using [^{31}P, ^{31}P] EXSY experiments.

	$\mathbf{M_{23}}$	**1**
$\Delta H^{\ddagger}$ /kcal mol^{-1}	27 ± 1	26 ± 1
$\Delta S^{\ddagger}$ /cal K^{-1} mol^{-1}	21 ± 4	19 ± 1
$\Delta G^{\ddagger}$ /kcal mol^{-1}	21 ± 2	20 ± 1

Table 3. Activation parameters for $\mathbf{M_{23}}$, **1** and **2** determined by reaction with butyl vinyl ether.

	$\mathbf{M_{23}}$	**1**	**2**
$\Delta H^{\ddagger}_{288.2\ K}$ /kcal mol^{-1}	25 ± 2	24 ± 2	23 ± 4
$\Delta S^{\ddagger}_{288.2\ K}$ /cal K^{-1} mol^{-1}	14 ± 9	11 ± 5	1 ± 11
$\Delta G^{\ddagger}_{288.2\ K}$ /kcal mol^{-1}	21 ± 4	21 ± 2	22 ± 5
k_{init} (288.2 K) /s^{-1}	5.56 x 10^{-5}	6.01 x 10^{-5}	8.49 x 10^{-4}

Metathesis Activity

The activities of $\mathbf{M_{23}}$ and **1** were evaluated in a series of metathesis reactions. Complex **2** is already known to be a poor metathesis complex from our earlier study of IPr- and IPr*-bearing complexes,[19] so was not evaluated further. To fully compare the activity of $\mathbf{M_{23}}$, evaluate the limits of this catalyst and draw out differences in activity between $\mathbf{M_{23}}$ and **1**, the efficiency of these catalysts was evaluated at low catalyst loadings (100 – 500 ppm) (**Table 4**).[38, 39] As shown in the table, it is possible to achieve the RCM of less hindered substrates using only 100 ppm of the ruthenium catalyst. As the steric bulk around the reacting alkene termini is increased, the reactivity drops slightly, requiring the use of slightly higher pre-catalyst loadings. Interestingly, complex **1** performs slightly better than $\mathbf{M_{23}}$ for substrates with very little steric bulk, although differences in reactivity are relatively small, but performs more poorly when steric bulk is added (e.g. entries 1 and 2, where simple methylation of one alkene leads to a four-fold drop in conversion). On balance, $\mathbf{M_{23}}$ still appears to be the more useful pre-catalyst. The highest TON achieved for $\mathbf{M_{23}}$ is with substrate **3**, reaching 32% conversion at 20 ppm of catalyst loading in only 1 h (TON 1.6 x 10^6 and TOF 4.4 x 10^3 sec^{-1}). In TON terms, this makes $\mathbf{M_{23}}$ one of the best catalysts for the RCM of less hindered substrates. Notably, a low pre-catalyst loading not only has cost benefits, but simplifies purification, particularly if high-purity pharmaceuticals or materials are being prepared; the use of 100 ppm of ruthenium catalyst to prepare a molecule of mass 500 g mol^{-1} would render the ruthenium content only 20 mg/kg (20 ppm) before work-up and any purification steps.

In cross-metathesis reactions at low pre-catalyst loading, the activity of the two catalysts is very similar in terms of both stereoselectivity and activity (**Table 5**). A greater than 20:1 *E*/*Z* ratio was achieved in each reaction. Interestingly, **1** appears to be slightly more selective for the formation of the dimer product in entry 2, which might be due to slightly more steric bulk, although this is quite far removed from the alkene terminus.

Due to the high activity of $\mathbf{M_{23}}$ with different substrates at low catalyst loadings, and therefore the potential utility in industrial applications, different solvents have been evaluated at low catalyst loadings using substrate **3** as a model. Many industries, particularly the pharmaceutical industry, are reducing their usage of less acceptable solvents (such as DCM) and replacing them with more environmentally-friendly alternatives.[40-42] As can be seen in **Table 6**, $\mathbf{M_{23}}$ shows excellent compatibility with green solvents, and can be used under neat conditions (bold entries), accessing product **4** quantitatively and with very low catalyst loadings in solvents such as methyl *iso*-butyl ketone.

While these experiments are a good indication of the outcomes of some prototypical metathesis reactions, further information on the comparison of $\mathbf{M_{23}}$ and **1** was desired. Therefore, kinetic experiments were carried out, in which the RCM of **3** to form **4** (catalysed by each complex) was monitored by ^{1}H NMR spectroscopy (0.5 mol L^{-1} **3** in toluene-d_8, catalysed by 250 ppm $\mathbf{M_{23}}$ or **1**, at 288 K). Concentration *versus* time profiles for the reactions can be found in **Figure 4(a)**. Only a

Table 4. Evaluation of 1 and M_{23} at low catalyst loadings, for model ring-closing olefin and enyne metathesis reactions.[a]

Entry	Substrate	Product	Cat	Loading	Conv
1	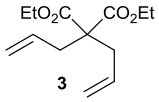 **3**	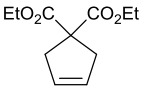 **4**	1	100 ppm	92%
			M_{23}	100 ppm	93%
2	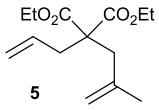 **5**	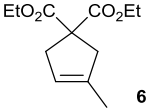 **6**	1	100 ppm	25%
			M_{23}	100 ppm	>99%
3	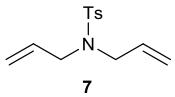 **7**	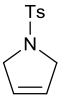 **8**	1	100 ppm	>99%
			M_{23}	100 ppm	96%
4	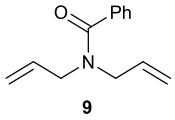 **9**	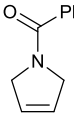 **10**	1	100 ppm	37%
			M_{23}	100 ppm	80%
5	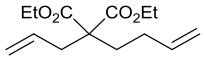 **11**	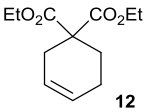 **12**	1	150 ppm	>99%
			M_{23}	200 ppm	89%
7	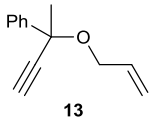 **13**	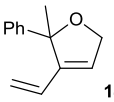 **14**	1	500 ppm	80%
			M_{23}	500 ppm	>99%
8	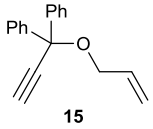 **15**	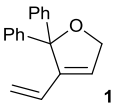 **16**	1	500 ppm	83%
			M_{23}	500 ppm	74%
6	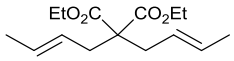 **17**	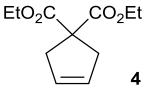 **4**	1	500 ppm	93%
			M_{23}	500 ppm	89%

[a] Reaction conditions: substrate (0.25 mmol), Ru complex, 0.5 mL DCM (0.5 mol L^{-1}), under argon at room temperature (*ca.* 25 °C) in a pierced vial in the glovebox for 1 h. [b] Conversions determined by ^{1}H NMR spectroscopy; average of two experiments.

Table 5. Evaluation of 1 and M_{23} at low catalyst loadings for model cross-metathesis reactions.[a]

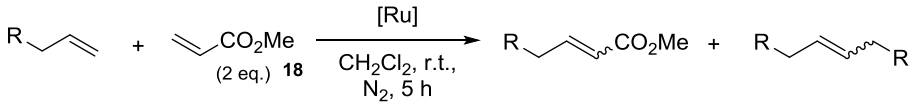

Entry	Substrate	Cat	Loading	CM product (%)	Dimer (%)	*E/Z* ratio
1	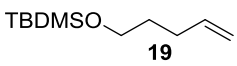 **19**	1	500 ppm	51	3	>20:1
		M_{23}	500 ppm	34	2	>20:1
2	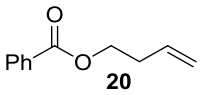 **20**	1	250 ppm	50	23	>20:1
		M_{23}	250 ppm	54	13	>20:1

[a] Reaction conditions: substrate (0.25 mmol), [Ru] complex, 0.5 mL DCM (0.5 mol L^{-1}), under argon at room temperature (*ca*. 25 °C) in a pierced vial in the glovebox for 5 h. [b] Conversions determined by ^{1}H NMR; average of two experiments.

Table 6. Evaluation of complex M_{23} at low catalyst loadings in a number of solvents.[a]

Entry	Solvent	[M_{23}] (ppm)	Conv. (%)
1	acetone	500	>99
2		100	97
3	CPME	500	>99
4		100	>99
5	DCM	500	>99
6		100	>99
7	1,2-DME	500	>99
8	1,4-dioxane	500	18
9	*iso*propanol	500	55
10	methyl *iso*-	500	>99
11	butyl ketone	100	99
11	2-methyltetra-	500	>99
12	hydrofuran	100	79
13	MTBE	500	>99
14	THF	500	>99
15	toluene	500	>99
16		100	>99
17	neat	500	>99
18		100	98

[a] Reaction conditions: 3 (0.25 mmol), M_{23}, 0.5 mL DCM (0.5 mol L^{-1}), under argon at room temperature (*ca*. 25 °C) in a pierced vial in the glovebox for 1 h. Conversions determined by ^{1}H NMR; average of two experiments.

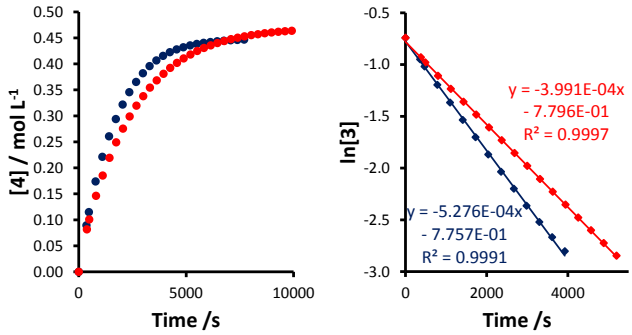

Figure 4. Kinetic data for the RCM of 3 (0.5 mol L^{-1}, toluene-d_8, 288 K with 250 ppm pre-catalyst), monitored by ^{1}H NMR spectroscopy: (a) concentration/time profiles; (b) first order treatment of kinetic data; SIPr in blue, SIPr^{OMe} in red.

modest difference in RCM rate was encountered. Treatment of the first three half-lives of kinetic data revealed excellent first order behaviour. Rate constants for the reactions could be extracted (k_{obs} = 5.28 x 10^{-4} s^{-1} for $\mathbf{M_{23}}$; k_{obs} = 3.99 x 10^{-4} s^{-1} for **1**) (**Figure 4 (b)**).

DFT Calculations

The use of DFT calculations to explore the potential energy surfaces of metathesis reactions is potentially very valuable, assisting in the rationalisation of reaction outcomes (both in terms of pre-catalyst design and substrate structure).[43-45] Metathesis is a complex sequence of multiple steps, rendering it rather difficult to experimentally study key steps in isolation. In addition, these methods hold promise for the prediction of the efficacy of complexes that have not yet been synthesised.

The potential energy surfaces (PESs) were modelled for the reactions of three complexes with ethene: $\mathbf{M_{23}}$, **1** and complex **21** which bears *para*-nitro substituents on the NHC aryl rings (which has not yet been synthesised) (**Figure 5**). The latter PES was explored to identify whether the synthesis of a less electron-rich system might be advantageous, as well as to identify any key trends. Notably, energy differences between intermediates with different aryl ring substituents are rather small (0.7 – 3.5 kcal mol^{-1}). The SIPr^{OMe} complex **1** is predicted to initiate slightly faster than $\mathbf{M_{23}}$, in agreement with experiments, with an upper barrier 0.4 kcal mol^{-1} lower in energy than for **1**. Furthermore, we conducted calculations with complex **21**, for which the upper barrier increases by 1.4 kcal mol^{-1}, demonstrating that more electron-donating groups in the *para* position of the *N*-aryl rings lead to slightly faster initiation. Bearing in mind the electronic nature of this trend, previously reported by Cavallo *et al.*,[33] we confirmed that the sterics of the NHC ligand are not modified by the substitution of the *N*-aryl ring; all three NHCs are within a narrow window of %V_{bur} that covers only 0.4%. Previous estimates of the error in %V_{bur} suggest that only differences of *ca.* 2% or more are meaningful.[23]

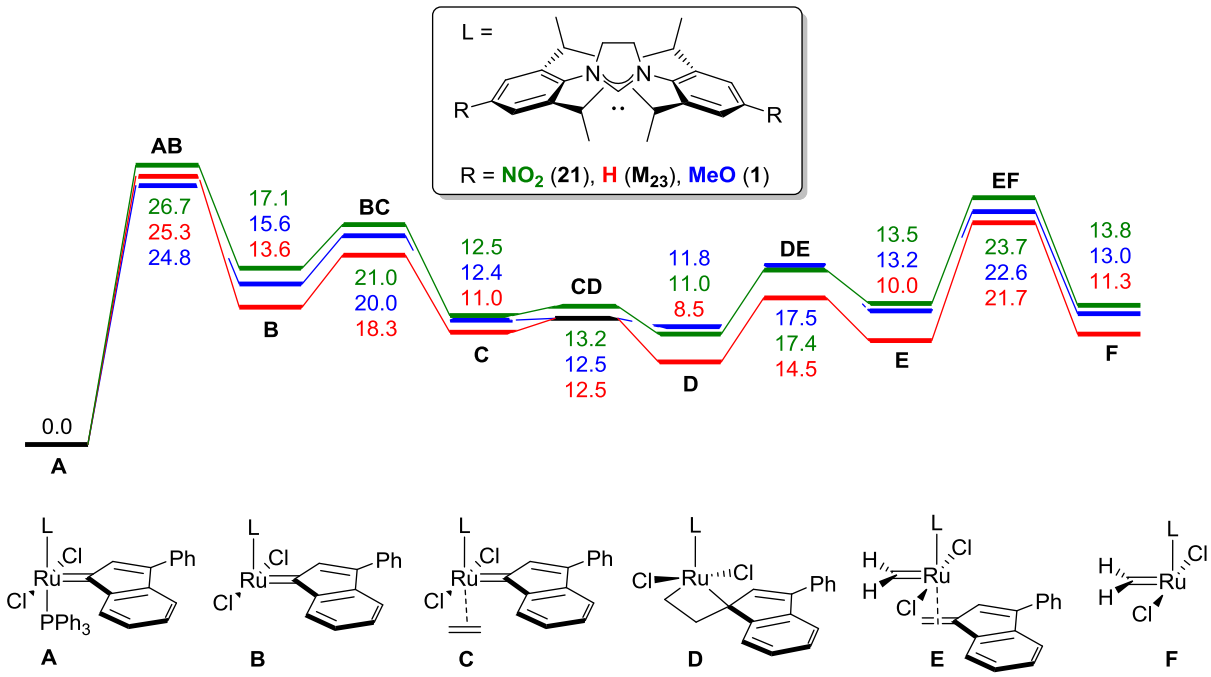

Figure 5. PESs for the metathesis of ethene by **1**, $\mathbf{M_{23}}$ and **21**.

However, other key intermediates on the PES, such as η^2-complexes and MCBs, are higher in energy (with respect to the pre-catalyst) for the *para*-substituted analogues, as are the barriers between these species which may explain the poorer performance of **1** in some metathesis reactions. The differences are typically very small, suggesting that *para*-substitution of the NHC aryl rings of SIPr-type NHCs is not a promising way in which to develop new and more active series of pre-catalysts.

Conclusions

In conclusion we report the synthesis of a derivative ruthenium complex bearing a *para*-methoxy substituted SIPr ligand and compared its reactivity with the SIPr-bearing analogue $\mathbf{M_{23}}$. Both complexes are able to catalyse RCM of less hindered olefins at very low catalyst loadings and are compatible with a range of solvents, including a number of solvents that are acceptable on scale in industrial applications. In particular, $\mathbf{M_{23}}$ delivers the best activity across a range of substrates. Even though the difference in properties between **1** and $\mathbf{M_{23}}$ is minimal, the two complexes show differences in reactivity. Complex **1** proved to be more influenced by the steric environment than $\mathbf{M_{23}}$. DFT calculations showed that differences between SIPr and $SIPr^{OMe}$-based catalysts were typically very small, with the latter ligand favouring a slight increase in initiation rate, but rendering intermediate species generally higher in energy. NHCs such as $SIPr^{OMe}$ are therefore unlikely to bring benefits to the field of metathesis.

Acknowledgements

SPN thanks the ERC (Advanced Investigator Award 'FUNCAT'), the EU (Seventh Framework Programme Project 'EUMET'), and the EPSRC for funding. SPN is a Royal Society Wolfson Merit Award holder. AP thanks the Spanish MINECO for a Ramón y Cajal contract (RYC-2009-05226) and European Commission for a Career Integration Grant (CIG09-GA-2011-293900).

Experimental

General information:

All reagents were used as received. Dichloromethane and toluene were dispensed from a solvent purification system from MBraun. Catalyst syntheses were performed in a MBraun glovebox containing dry Ar and less than 1 ppm oxygen. ^{1}H, ^{31}P{^{1}H}, and ^{13}C{^{1}H} Nuclear Magnetic Resonance (NMR) spectra were recorded on Bruker Avance 300 or Bruker Avance II 400 Ultrashield NMR spectrometers. The EXSY experiments were recording using the previous procedure. $\mathbf{M_{23}}$ was purchased from Umicore and used as received. Compound **19** was synthesised in accordance with the reported procedure. Elemental analyses were performed at the London Metropolitan University. Solvents were dried and degassed according to the literature. SIPr^{OMe} was synthesised according to the previously reported procedure. Substrates **1**, **3**, **4**, **5**, **7**, **9**, **11**, **13**, **15**, **17**, **20**, **21** and products **2**, **4**, **6**, **8**, **10**, **12**, **14** and **18** have previously been described in the literature.[1-3]

Synthesis of [RuCl$_2$(SIPr^{OMe})(PPh$_3$)(3-phenylindenylidene)](1):

In the glovebox, $\mathbf{M_{10}}$ (1.00 g, 1.13 mmol) and SIPr^{OMe} (914 mg, 1.2 mmol)) were charged to a Schlenk flask and dissolved in toluene (3 mL). The reaction was taken out of the glovebox and stirred at 40 °C for 5 h under Ar. After this time, the mixture was allowed to cool to RT and the solvent was removed under vacuum. The remaining solid was recrystallised from a mixture of dichloromethane / pentane. The mixture was filtered, washed with cold methanol (2 x 5 mL) and cold hexane (8 x 25 mL), affording [RuCl$_2$(SIPr^{OMe})(PPh$_3$)(3-phenylindenylidene)] (**1**) (750 mg, 0.49 mmol, 44%) as a microcrystalline solid. ^{1}H NMR (C_6D_6, 400 MHz): δ = 8.04 (d, J = 7.2 Hz, 1 H), 7.74 (d, J = 7.9 Hz, 2H), 7.38 (m, 8H), 7.21 (m, 2H), 6.92 (m, 16H), 6.83 (d, J = 3.2 Hz, 1H), 6.63 (m, 1H), 6.45 (d, J = 2.9 Hz, 1H), 6.26 (d, J = 2.9 Hz, 1H), 3.53 (s, 3H) 3.10 (s, 3H) 1.77 (d, J = 6.5 Hz, 3H), 1.57 (d, J = 6.5 Hz, 3H), 1.77 (d, J = 6.5 Hz, 3H) 1.20 (m, 13H) 0.85 (m, 9H) ppm. ^{13}C{^{1}H} NMR (CD_2Cl_2, 75 MHz): δ = 299.9, 160.9, 159.9, 152.2, 151.5, 149.9, 149.2, 143.0, 141.3, 140.8, 139,3, 137.2, 135.1, 132.1, 131.7, 130.9, 130.7, 129.3, 129.3, 129.1, 127.0, 116.1, 110.6, 110.4, 108.7, 116.7, 55.2, 54.7, 54.2, 34.2 30.4, 29.4, 29.0 27.8, 27.2, 27.0, 26.9, 25.8, 24.2, 24.0, 23.9, 22.7, 22.3 ppm. ^{31}P{^{1}H} NMR (162 MHz, C_6D_6) δ = 29.89 ppm. Anal. Calcd for $C_{62}H_{67}Cl_2N_2O_2PRu$ C, 69.26; H, 6.28; N 2.61; Found: C, 69.10; H, 6.37; N, 2.70.

General procedure for RCM and Enyne reactions:

Inside the glovebox stock solutions were prepared of substrate (2.5 mmol/1 mL) and catalyst (0.025 mmol/4 mL) in the appropriate solvent. An aliquot of substrate was then measured into a 4 mL vial, then a volume of the same solvent required to reach a concentration of 0.5 M was added, followed by a corresponding aliquot of the catalyst to reach the desired catalyst loading. The reaction was stirred for 1 h and ^{1}H NMR of the reaction mixture was recorded to determine conversion.

General procedure for CM reactions:

Inside the glovebox stock solutions were prepared of substrate (2.5 mmol/1 mL) and catalyst (0.025 mmol/4 mL) in the appropriate solvent. An aliquot of substrate was then measured into a 4 mL vial, then a volume of the same solvent required to reach a concentration of 0.5 M was added, followed with a corresponding aliquot of the catalyst to reach the desired catalyst loading. After this, two equivalents of the electron poor olefin (0.5 mmol) were added. The progress of the reaction was monitored by ^{1}H NMR. At reaction completion solvent was removed under vacuum and the crude residue was checked by ^{1}H NMR. Conversion was determined by ^{1}H NMR spectroscopy by integrating the characteristic signals for allylic proton resonances.

NMR initiation kinetics with butyl vinyl ether:

Inside a glovebox, 400 μL of a stock solution of complex in toluene-d_8 (0.0106 mmol/400 μL; 0.1325 mmol/5 mL) and an amount of toluene-d_8 so that the total volume of the solution after addition of butyl vinyl ether was 600 μL were introduced into a screw-cap NMR tube. The solution was left to equilibrate at the desired temperature, and then the butyl vinyl ether (in equivalents relative to [Ru]) was injected into the solution; the progress of the reaction was followed by ^{31}P{^{1}H} and ^{1}H NMR every 10 min.

Supporting Information

Electronic Supplementary Information (ESI) available: Characterisation data for new complexes and details of catalytic experiments. See DOI: 10.xxxx/xxx/. Crystallographic data can be obtained from the Cambridge Crystallographic Data Centre for **1** (999049) and $\mathbf{M_{23}}$ (999050) free of charge *via* their website at www.ccdc.cam.ac.uk/data_request/cif.

References

1. W. A. Herrmann, *Angew. Chem. Int. Ed.*, 2002, **41**, 1290-1309.
2. S. Díez-González, N. Marion and S. P. Nolan, *Chem. Rev.*, 2009, **109**, 3612-3676.
3. D. J. Nelson and S. P. Nolan, *Chem. Soc. Rev.*, 2013, **42**, 6723-6753.

4. H. Clavier and S. P. Nolan, *Chem. Commun.*, 2010, **46**, 841-861.
5. T. Dröge and F. Glorius, *Angew. Chem. Int. Ed.*, 2010, **49**, 6940-6952.
6. S. P. Nolan, *Acc. Chem. Res.*, 2011, **44**, 91-100.
7. G. C. Fortman and S. P. Nolan, *Chem. Soc. Rev.*, 2011, **40**, 5151-5169.
8. G. C. Vougioukalakis and R. H. Grubbs, *Chem. Rev.*, 2009, **110**, 1746-1787.
9. C. Samojlowicz, M. Bieniek and K. Grela, *Chem. Rev.*, 2009, **109**, 3708-3742.
10. F. Boeda, H. Clavier and S. P. Nolan, *Chem. Commun.*, 2008, 2726-2740.
11. J. Huang, E. D. Stevens, S. P. Nolan and J. L. Petersen, *J. Am. Chem. Soc.*, 1999, **121**, 2674-2678.
12. M. Scholl, S. Ding, C. W. Lee and R. H. Grubbs, *Org. Lett.*, 1999, **1**, 953-956.
13. T. Ritter, A. Hejl, A. G. Wenzel, T. W. Funk and R. H. Grubbs, *Organometallics*, 2006, **25**, 5740-5745.
14. M. Bieniek, A. Michrowska, D. L. Usanov and K. Grela, *Chem. Eur. J.*, 2008, **14**, 806-818.
15. M. S. Sanford, J. A. Love and R. H. Grubbs, *J. Am. Chem. Soc.*, 2001, **123**, 6543-6554.
16. B. F. Straub, *Angew. Chem. Int. Ed.*, 2005, **44**, 5974-5978.
17. S. H. Hong, A. G. Wenzel, T. T. Salguero, M. W. Day and R. H. Grubbs, *J. Am. Chem. Soc.*, 2007, **129**, 7961-7968.
18. C. A. Urbina-Blanco, A. Leitgeb, C. Slugovc, X. Bantreil, H. Clavier, A. M. Z. Slawin and S. P. Nolan, *Chem. Eur. J.*, 2011, **17**, 5045-5053.
19. S. Manzini, C. A. Urbina Blanco, A. M. Z. Slawin and S. P. Nolan, *Organometallics*, 2012, **31**, 6514-6517.
20. C. A. Tolman, *Chem. Rev.*, 1977, **77**, 313-348.
21. A. Poater, B. Cosenza, A. Correa, S. Giudice, F. Ragone, V. Scarano and L. Cavallo, *Eur. J. Inorg. Chem.*, 2009, **2009**, 1759-1766.
22. D. J. Nelson, S. Manzini, C. A. Urbina-Blanco and S. P. Nolan, *Chem. Commun.*, 2014, **50**, 10355-10375.
23. D. Nelson, A. Collado, S. Manzini, S. Meiries, D. B. Cordes, A. M. Z. Slawin and S. P. Nolan, *Organometallics*, 2014, In Press.
24. S. Meiries, K. Speck, D. B. Cordes, A. M. Z. Slawin and S. P. Nolan, *Organometallics*, 2012, **32**, 330-339.
25. G. Le Duc, S. Meiries and S. P. Nolan, *Organometallics*, 2013, **32**, 7547-7551.
26. S. Leuthäußer, D. Schwarz and H. Plenio, *Chem. Eur. J.*, 2007, **13**, 7195-7203.
27. C. A. Urbina-Blanco, S. Manzini, J. P. Gomes, A. Doppiu and S. P. Nolan, *Chem. Commun.*, 2011, **47**, 5022-5024.
28. S. Meiries and S. P. Nolan, *Synlett*, 2014, **25**, 393-398.
29. S. Fantasia, J. L. Petersen, H. Jacobsen, L. Cavallo and S. P. Nolan, *Organometallics*, 2007, **26**, 5880-5889.
30. O. Back, M. Henry-Ellinger, C. D. Martin, D. Martin and G. Bertrand, *Angew. Chem. Int. Ed.*, 2013, **52**, 2939-2943.
31. A. Liske, K. Verlinden, H. Buhl, K. Schaper and C. Ganter, *Organometallics*, 2013, **32**, 5269-5272.
32. R. Dorta, E. D. Stevens, N. M. Scott, C. Costabile, L. Cavallo, C. D. Hoff and S. P. Nolan, *J. Am. Chem. Soc.*, 2005, **127**, 2485-2495.
33. C. A. Urbina-Blanco, A. Poater, T. Lebl, S. Manzini, A. M. Z. Slawin, L. Cavallo and S. P. Nolan, *J. Am. Chem. Soc.*, 2013, **135**, 7073-7079.
34. S. Leuthäußer, V. Schmidts, C. M. Thiele and H. Plenio, *Chem. Eur. J.*, 2008, **14**, 5465-5481.
35. R. Credendino, L. Falivene and L. Cavallo, *J. Am. Chem. Soc.*, 2012, **134**, 8127-8135.
36. H.-C. Yang, Y.-C. Huang, Y.-K. Lan, T.-Y. Luh, Y. Zhao and D. G. Truhlar, *Organometallics*, 2011, **30**, 4196-4200.
37. J. Louie and R. H. Grubbs, *Organometallics*, 2002, **21**, 2153-2164.
38. L. H. Peeck, R. D. Savka and H. Plenio, *Chem. Eur. J.*, 2012, **18**, 12845-12853.
39. R. Kadyrov, *Chem. Eur. J.*, 2013, **19**, 1002-1012.
40. R. K. Henderson, C. Jimenez-Gonzalez, D. J. C. Constable, S. R. Alston, G. G. A. Inglis, G. Fisher, J. Sherwood, S. P. Binks and A. D. Curzons, *Green Chem.*, 2011, **13**, 854-862.

41. K. Alfonsi, J. Colberg, P. J. Dunn, T. Fevig, S. Jennings, T. A. Johnson, H. P. Kleine, C. Knight, M. A. Nagy, D. A. Perry and M. Stefaniak, *Green Chem.*, 2008, **10**, 31-36.
42. D. Prat, O. Pardigon, H.-W. Flemming, S. Letestu, V. Ducandas, P. Isnard, E. Guntrum, T. Senac, S. Ruisseau, P. Cruciani and P. Hosek, *Org. Proc. Res. Dev.*, 2013.
43. R. Credendino, A. Poater, F. Ragone and L. Cavallo, *Cat. Sci. Technol.*, 2011, **1**, 1287-1297.
44. I. H. Hillier, S. Pandian, J. M. Percy and M. A. Vincent, *Dalton Trans.*, 2011, **40**, 1061-1072.
45. A. Poater, N. Bahri-Laleh and L. Cavallo, *Chem. Commun.*, 2011, **47**, 6674-6676.